


ORIGINAL ARTICLE

Conditional loss of *Engrailed1/2* in *Atoh1*-derived excitatory cerebellar nuclear neurons impairs eupneic respiration in mice

Angela P. Taylor¹ | Andrew S. Lee^{2,3} | Patricia J. Goedecke⁴ |
Elizabeth A. Tolley⁴ | Alexandra L. Joyner^{2,3,5} | Detlef H. Heck¹ 

¹Department of Anatomy and Neurobiology, College of Medicine, University of Tennessee Health Science Center, Memphis, Tennessee, USA

²Developmental Biology Program, Sloan Kettering Institute, New York, New York, USA

³Neuroscience Program, Weill Cornell Graduate School of Medical Sciences, New York, New York, USA

⁴Division of Biostatistics, Department of Preventive Medicine, College of Medicine, University of Tennessee Health Science Center, Memphis, Tennessee, USA

⁵Biochemistry, Cell and Molecular Biology Program, Weill Cornell Graduate School of Medical Sciences, New York, New York, USA

Correspondence

Detlef H. Heck, Department of Anatomy and Neurobiology, College of Medicine, University of Tennessee Health Science Center, 855 Monroe Ave, Suite 515 Memphis, TN 38163, USA.
Email: dheck@uthsc.edu

Funding information

National Cancer Institute Cancer Center, Grant/Award Number: P30 CA008748-48; National Institute of Mental Health, Grant/Award Numbers: NIMH R37MH085726, NICHD T32HD060600, NIMH F31MH122068, NIMH R01MH112143; Neuroscience Institute of the University of Tennessee Health Science Center (UTHSC)

Abstract

Evidence for a cerebellar role during cardiopulmonary challenges has long been established, but studies of cerebellar involvement in eupneic breathing have been inconclusive. Here we investigated temporal aspects of eupneic respiration in the *Atoh1-En1/2* mouse model of cerebellar neuropathology. *Atoh1-En1/2* conditional knockout mice have conditional loss of the developmental patterning genes *Engrailed1* and *2* in excitatory cerebellar nuclear neurons, which leads to loss of a subset of medial and intermediate excitatory cerebellar nuclear neurons. A sample of three *Atoh1*-derived extracerebellar nuclei showed no cell loss in the conditional knockout compared to control mice. We measured eupneic respiration in mutant animals and control littermates using whole-body unrestrained plethysmography and compared the average respiratory rate, coefficient of variation, and the CV2, a measure of intrinsic rhythmicity. Linear regression analyses revealed that *Atoh1-En1/2* conditional knockouts have decreased overall variability ($p = 0.021$; $b = -0.045$) and increased intrinsic rhythmicity compared to their control littermates ($p < 0.001$; $b = -0.037$), but we found no effect of genotype on average respiratory rate ($p = 0.064$). Analysis also revealed modestly decreased respiratory rates ($p = 0.025$; $b = -0.82$), increased coefficient of variation ($p = 0.0036$; $b = 0.060$), and increased CV2 in female animals, independent of genotype ($p = 0.024$; $b = 0.026$). These results suggest a cerebellar involvement in eupneic breathing by controlling rhythmicity. We argue that the cerebellar involvement in controlling the CV2 of respiration is indicative of an involvement of coordinating respiration with other orofacial rhythms, such as swallowing.

KEYWORDS

Atoh1, breathing rhythm, cerebellar development, cerebellar nuclei, cerebellum, conditional knock out, *Engrailed 1* and *2*, eupneic respiration, excitatory cerebellar nuclear neurons, interposed nucleus, mouse, plethysmography

1 | INTRODUCTION

The involvement of the cerebellum in cardiopulmonary function such as blood pressure regulation and respiration has long been established and

is evidenced by a wealth of anatomical and neuropathological data.^{1–10} There is a clear cerebellar role in breathing during respiratory challenges, like hunger for air and hypoxia, but a similar relationship could not be found during normal breathing (eupneic breathing or eupnea).^{8,11–14}

This is an open access article under the terms of the Creative Commons Attribution-NonCommercial-NoDerivs License, which permits use and distribution in any medium, provided the original work is properly cited, the use is non-commercial and no modifications or adaptations are made.

© 2021 The Authors. Genes, Brain and Behavior published by International Behavioural and Neural Genetics Society and John Wiley & Sons Ltd.

However, recent studies have successfully focused on cerebellar involvement in specifically the temporal aspects of eupneic respiration,^{15–17} as temporal coordination is one of the key functions assigned to the cerebellum.¹⁸ We recently investigated temporal aspects of eupneic respiration in a mouse model with Purkinje cell (PC) silencing.¹⁵ This mouse model lacked synaptic vesicle transmission selectively in PCs, effectively eliminating transmission of cerebellar cortical output to the cerebellar nuclei.¹⁹ The average respiratory rate and coefficient of variation (CV) of the inter-respiratory intervals (IRI) were not significantly affected by loss of PC transmission; however mutant animals exhibited an increase in CV2, a measure of intrinsic rhythmicity which compares neighboring IRIs.^{15,20} This result suggested a cerebellar role in controlling temporal aspects of eupneic respiration.

Here we investigate the role of excitatory cerebellar nuclei neurons (eCN) in controlling eupneic respiration. The eCN integrate synaptic inputs from PCs as well as climbing fiber and mossy fiber collaterals and are the final output neurons of the cerebellum.^{18,21,22} ECN project widely throughout the midbrain and hindbrain. Fujita et al. recently identified over 60 regions, including premotor nuclei involved in respiratory control, targeted by the excitatory neurons of the fastigial (medial) nucleus alone using fluorescent anterograde tracers in mice.²³ Several other studies have implicated brain stem nuclei with respiratory function as potential targets of the eCN, including the Kölliker-Fuse nucleus, parabrachial complex, and lateral reticular nucleus.^{23,24} Lu et al. have previously shown that there are robust projections from medial cerebellar nuclei (mCN) and some projections from intermediate CN to the ventromedial reticular formation, a structure involved in respiratory and orofacial motor control.^{16,25–28} In addition, they reported that a subset of mCN neurons have firing patterns which were correlated with respiration, fluid licking and whisker movements.¹⁶

To address the role of the eCN in eupneic breathing we used a mouse model with conditional loss of the developmental patterning genes *Engrailed1/2* (*En1/2*) in neurons that express *Atonal homolog 1* (*Atoh1*) during development, which includes eCN and granule cells. This results in partial loss of the eCN in the medial and intermediate CN but a near normal cerebellar cytoarchitecture despite a smaller cerebellum size.²⁹ *En1/2* encode homeobox transcription factors which have been shown to be expressed in and essential for several aspects of mid/hindbrain development.^{30–32} Furthermore, mutant mice have revealed that *En1/2* are crucial in the cerebellum for normal molecular patterning of the PC parasagittal stripes, foliation, and afferent circuit maps.^{33–35}

The conditional mouse model used here (*Atoh1-En1/2* CKOs) uses a *Cre/lox* system to conditionally knock out *En1/2* in rhombic lip-derived neurons using the *Atoh1* promoter. Upper and lower rhombic lip progenitor cells express the transcription factor ATOH1 and give rise to the glutamatergic neurons of the cerebellum, in addition to pre-cerebellar nuclei neurons. In terms of cerebellar size and foliation, *Atoh1-En1/2* CKOs suffer proportional scaling down of neuron numbers in hypoplastic lobules of the anterior and central vermis and paravermis.^{29,32} In addition, the number of eCN in the medial (mCN) and intermediate CN is reduced in mutants by about half.³² This is of particular relevance to our study, as the posterior mCN that is reduced in

mutants projects to several premotor brain stem nuclei involved in respiratory function and orofacial control.^{23,36} Despite the loss of eCN, the cytoarchitecture of the cerebellar cortex is well maintained in mutants, setting this model apart from most other cerebellar mutants and making it ideal for our investigation. The *Atoh1-En1/2* CKOs have also been shown to have motor behavioral deficits,^{29,32} but eupneic breathing has not been studied.

2 | MATERIALS AND METHODS

2.1 | Animals

All animals were bred and genotyped in the lab of Dr. Alexandra Joyner (Memorial Sloan Kettering Cancer Center, New York, NY) and then transferred to the animal care facilities at the University of Tennessee Health Science Center where they were housed in groups of the same sex. Use of animals and all experimental procedures were performed under the approval of the Institutional Animal Care and Use Committee of University of Tennessee Health Science Center and Memorial Sloan Kettering Institute. In total, 39 animals were used for analysis (details in Table 1). The *Atoh1-En1/2* CKO mice²⁹ use a *Cre/lox* system and the *Atoh1* promoter to conditionally knock out the *Engrailed1/2* genes in rhombic lip-derived cells. Mutant animals (*Atoh1-Cre+*; *En1^{lox/lox}*; *En2^{lox/lox}*) were compared to their control littermates (*En1^{lox/lox}*; *En2^{lox/lox}*). We recorded animals at 4–5 months old, corresponding to mature adulthood in mice.³⁷ All experimental procedures involving animals were performed during the light phase of a 12-h light/dark cycle.

To examine the number of *Atoh1*-derived extracerebellar nuclei in the *Atoh1-En1/2* CKO mice, *Atoh1-En1/2* CKO mice with a Cre-dependent nuclear tdTomato reporter (*Ai75D*³⁸) were generated (*Atoh1-Cre/+*; *En1^{lox/lox}*; *En2^{lox/lox}*; *R26^{LSL-nls-tdTomato/+}*). Mice with *Atoh1-Cre* and *Ai75D* alleles were used as non-littermate controls (*Atoh1-Cre/+*; *R26^{LSL-nls-tdTomato/+}*). Four non-littermate controls and four *Atoh1-En1/2* CKOs at postnatal 30 were used for quantifications.

2.2 | Plethysmograph recording

We recorded respiration under eupneic conditions as described previously.¹⁵ In short, we used a plethysmograph chamber as shown in Figure 1A, consisting of an airtight container with constant air flow and a pressure transducer attached. Animals were recorded individually for 30–40 min. During recording an opaque covering was placed over the entire apparatus in order to provide a calming dark environment and reduce potential stressors. Pressure transducer output was recorded and digitized using an analogue-to-digital converter and Spike2 software (both Cambridge Electronic Design, Cambridge, UK). As the animal inhales, pressure inside the chamber increases slightly, causing the pressure transducer output voltage to increase (Figure 1B). Voltage peaks, corresponding to the end of inspiration, were marked and this time sequence of markers was used for all further analysis. Eupneic

TABLE 1 Mouse group composition and means. Shown are count and (%) or mean and (SD), respectively, depending on whether the variable is discrete or continuous

	All (N = 39)	Mutant (N = 19)	Control (N = 20)
Sex			
Female	24 (61.5%)	12 (30.8%)	12 (30.8%)
Male	15 (38.5%)	7 (17.9%)	8 (20.5%)
Mean IRI (s)	0.164 (0.035)	0.156 (0.030)	0.172 (0.039)
Rate (Hz)	6.30 (1.12)	6.58 (1.06)	6.03 (1.13)
CV	0.37 (0.06)	0.34 (0.07)	0.39 (0.06)
CV2	0.23 (0.04)	0.21 (0.03)	0.25 (0.03)

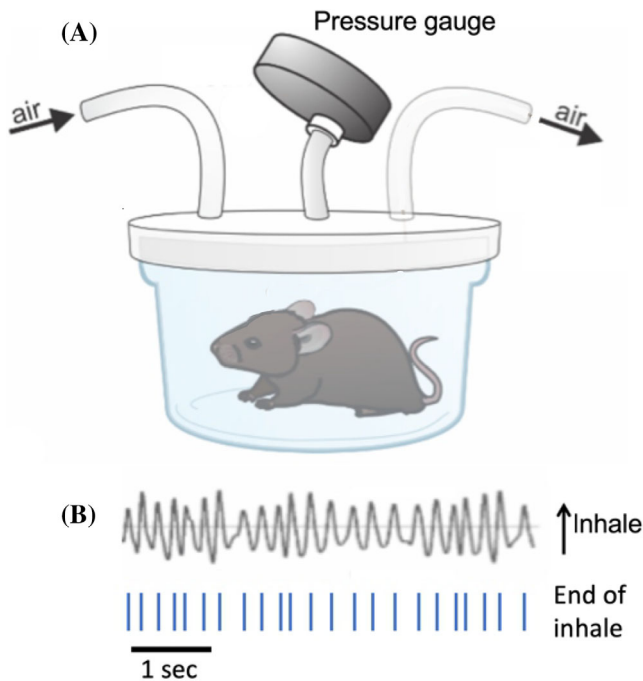


FIGURE 1 Whole-body unrestrained plethysmograph recording. (A) Custom-made plethysmograph chamber. Pressure changes due to respiration are measured by pressure transducer (Validyne Engineering) and reflected by voltage changes, shown in B. (B) Inhalation caused an increase in pressure in the plethysmograph chamber, which is reflected as an increase in the output voltage of the pressure transducer. The times of voltage peaks were marked, representing the end of inspiration. The sequence of these time markers was used for all further analysis

respiration analyzed here included breathing at rest and sniffing behavior, that is, respiratory frequencies between 1 and 16 Hz. Periods with respiratory intervals outside of the 1–16 Hz range as well as periods showing sharp increases or decreases in voltage which were outside the range of the transducer (clipping) were excluded from analysis. After each recording the plethysmograph chamber was cleaned with a 70% ethanol solution and allowed to dry.

2.3 | Tissue processing, microscopy, and image analysis

Mice were euthanized by ketamine/xylazine and then perfused transcardially with 1× PBS and then 4% paraformaldehyde. Brains

were dissected and post-fixed in the same fixatives overnight at 4°C and cryopreserved in 30% sucrose in 1× PBS for 2 days at 4°C. Brains were embedded in Tissue-Tek OCT compound (Sakura Finetek Co., Japan) and cryosectioned sagittally at 14 μm and directly mounted on glass slides.

Slides were processed for immunofluorescence using a procedure described previously.³² Slides were imaged using a slide scanner (NanoZoomer 2.0-HT, Hamamatsu Photonics, Bridgewater, NJ) and Cy3 channel for regions of interest were exported at 10× magnification. Parabrachial nucleus, lateral reticular nucleus and pons were cropped from images using Photoshop (Adobe, San Jose, CA) and saved as TIFF format. Using a batch “analyze particle” function on ImageJ (National Institute of Health, Bethesda, MD), cropped images were auto-thresholded and the number of nuclear tdTomato-positive cells were quantified. Every 10th section was quantified for the parabrachial and lateral reticular nuclei and every other section was used to quantify the pons. The number of sections quantified for each region of interest between non-littermate control and mutants were not different.

2.4 | Statistical analysis

The raw pressure transducer voltage signal was first processed using a software FIR Butterworth low pass filter with a cutoff at 20 Hz (Spike2) to remove noise without distorting the respiratory data, as suggested by Lim et al.³⁹ To remove very low frequency (<1 Hz) drift, the built-in Spike2 DC remove channel process was utilized (time constant = 0.1 s). Signal peaks were marked using a minimum interval of 0.06 s to exclude local maxima which do not correspond to the end of inspiration, given that murine respiratory rates vary from about 1–16 Hz (including sniffing behavior).^{40,41} Minimum peak height varied based on the amplitude of individual recordings, but ranged from 0.15 to 0.35 Volts. Inter-respiratory intervals (IRI) were determined by calculating the time between subsequent end-of-inspiration marks (Δt). CV was calculated as the SD of the IRI distribution divided by the mean. Finally CV2 which was first described by Holt et al. to analyze intrinsic variability of spiking activity in cat visual cortex neurons,²⁰ was calculated using (Equation 1):

$$CV2 = \frac{2 |\Delta t_{i+1} - \Delta t_i|}{\Delta t_{i+1} + \Delta t_i} \quad (1)$$

The average CV2 of a sequence of respiratory intervals is the mean of all CV2s calculated for each adjacent pair of IRIs.

Periods of high signal noise, which can be caused e.g. by the animal blocking the air in or outflow from the chamber, were excluded from analysis.³⁹ Thus for each mouse, the CV, CV2, and mean IRI of five respiratory sequences (each 60 s long) were calculated independently from noise-free data segments. Since data segments varied from mouse to mouse and given that respiratory rate and variability may vary as the animal acclimates to the plethysmograph chamber, segment start time (ST) was also included as a predictor in all analyses (i.e., if the sequence analyzed was the first 60 s of the recording, ST = 0 s). See Figures S1 and S2 for further discussion of ST. All calculations and statistical analyses were performed using MATLAB scripts (MathWorks, Natick, MA).

Response variables were tested to ensure that they were appropriate for linear regression. In the following tests for normality and homoscedasticity, data for each response variable were treated as a single group (for example, all CV data was grouped regardless of sex or strain). First, response variables were evaluated to ensure normality using quantile-quantile (QQ) plots, which compare the distribution of

a data set with the normal distribution. The Breusch-Pagan test was used to evaluate the data for homoscedasticity, where the null hypothesis is that data are homoscedastic and a p -value ≤ 0.05 indicates heteroscedasticity.^{42,43} To determine the effect of sex, strain, and ST on response variables (CV, CV2, and mean IRI), linear regression analysis was applied. Models were fitted to relate response variables to predictor variables (gender, strain, and ST). Nonsignificant predictor variables ($p \geq 0.05$) were removed to increase degrees of freedom and improve the model. Model fit was confirmed using residual plots.

For image analysis of immunostained tissue from extracerebellar nuclei, the total number of tdTomato-positive cells were compared between each region between genotypes using the non-parametric Mann-Whitney U test (GraphPad Prism v 9.2.0, GraphPad Software, San Diego, CA). One control animal was excluded from the lateral reticular nucleus quantifications as the number of sections containing the region of interest was not sufficient. Data are presented as box and whisker plots and “+” indicates the mean.

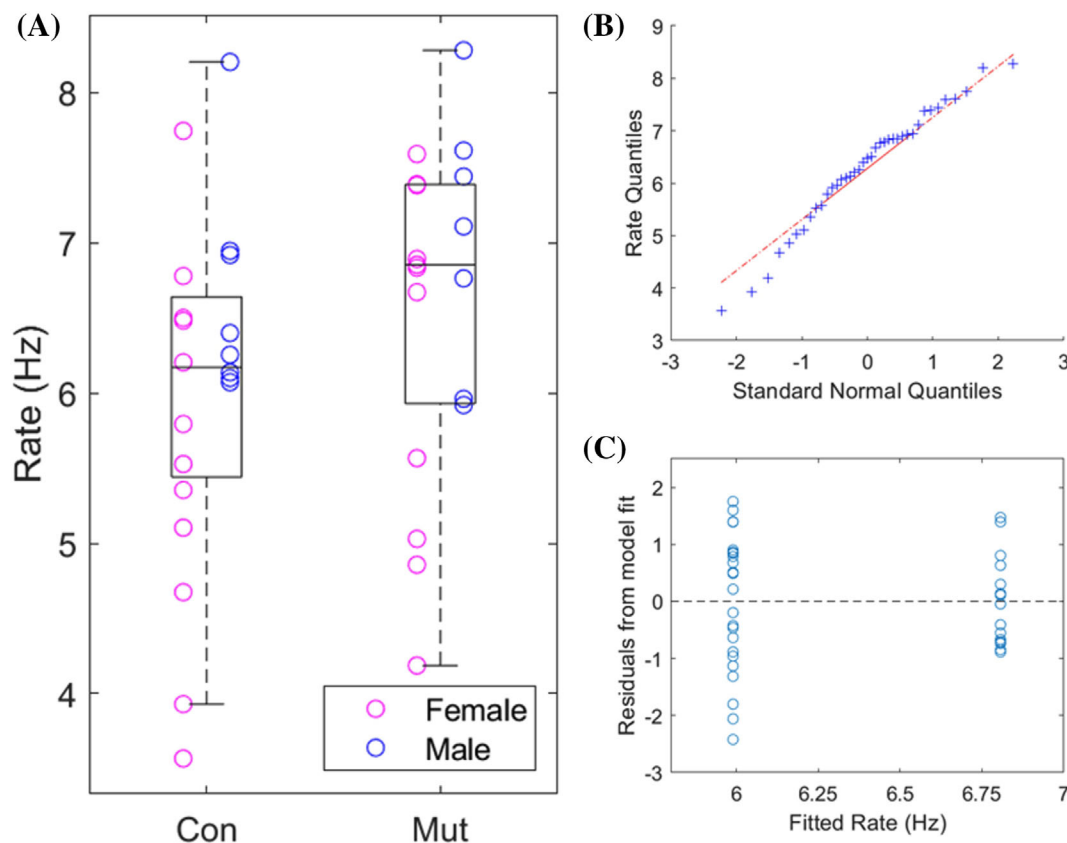


FIGURE 2 Average respiratory rate is influenced by sex and not genotype. (A) Boxplot showing the average respiratory rates of individual mice (open circles). There was no significant effect of genotype ($p = 0.064$) or ST ($p = 0.33$) on respiratory rate. After genotype and ST were removed from the model, sex remained a significant predictor of average rate ($p = 0.025$; $b = -0.82$). The upper, middle, and lower box limits indicate the 75th percentile, median, and 25th percentile, respectively. The whiskers represent $\pm 2.7\sigma$ encompassing 99.3% of the data if the data are normally distributed. (B) Quantile-quantile plot of rate data versus standard normal distribution. Blue “+” signs indicate quantiles, dotted red line represents the plot of the line if data has a perfectly normal distribution. (C) Plot of residuals versus fitted rate, based on the linear model with sex as the only predictor of rate. Ideally, residuals are distributed equally for both males and females with no clear trend. Actual data shows an apparent increased spread of residuals for female data as compared to males. Fitted rate values: all female, 5.99 Hz; all male, 6.81 Hz

3 | RESULTS

To evaluate whether conditional loss of *En1/2* in rhombic lip-derived neurons has an effect on average respiratory rate during eupnea, we first used mean IRI as the response variable as in Liu et al.¹⁵ However, the QQ plot of IRI data, as well as the total IRI distribution (including all IRIs instead of averages) both showed clear right skewness for both *Atoh1-En1/2* CKOs (*Atoh1-Cre/+; En1^{lox/lox}; En2^{lox/lox}* mice) and their littermate controls (*En1^{lox/lox}; En2^{lox/lox}* mice) (see Figure S3), indicating that the variable was not normally distributed. This could be due in part to the artificial IRI minimum of 0.06 s, which was enforced to exclude intervals which are physiologically impossible. In addition, the Breusch-Pagan test revealed that IRI data were not homoscedastic ($p = 0.044$). Because of this right skew and failure to meet standards of homoscedasticity, the IRI data could not satisfy the assumptions of linear regression. To improve the model, a nonlinear transformation was applied by using the reciprocal of the mean IRI, which in this case is the physiologically relevant measure of respiration rate. Again, a QQ plot and the Breusch-Pagan test were employed, revealing that respiration rate was homoscedastic ($p = 0.055$) and better approximated a normal distribution as seen in Figure 2B.

We found no significant effect of genotype or ST on average rate ($p = 0.064$ and 0.33 , respectively and adjusted for sex), so both variables were removed from the model to improve fit. Female animals showed significantly slower respiratory rates ($R^2 = 0.128$; $F_{1,37} = 5.45$; $t_{37} = -2.3$; $p = 0.025$; $b = -0.82 \pm 0.35$) than males, independent of genotype. This result was opposite to what we predicted in terms of sex, based on Liu et al.¹⁵ Raw residuals were plotted against fitted values, shown in Figure 2C, which revealed that female animals had greater residual variability than males. This can also be seen in the spread of rate values as shown in the boxplot in Figure 2A. Regardless, the effect of sex was modest, and average rates were 6.81 Hz for females and 5.99 Hz for males. Our hypothesis was supported, however, in that conditional loss of *En1/2* in the rhombic lip-derived neurons did not have a significant effect on average respiratory rate. To be sure that the effect of sex on rate did not influence CV or CV2, rate was initially included as a predictor variable in the remaining linear regressions. Rate was not significant in either case ($p > 0.05$, data not shown) so it was removed from both models.

Next, we investigated if the conditional loss of *En1/2* in rhombic lip-derived neurons affects eupneic respiratory variability using the coefficient of variation (CV) of IRIs. The QQ plot revealed that CV

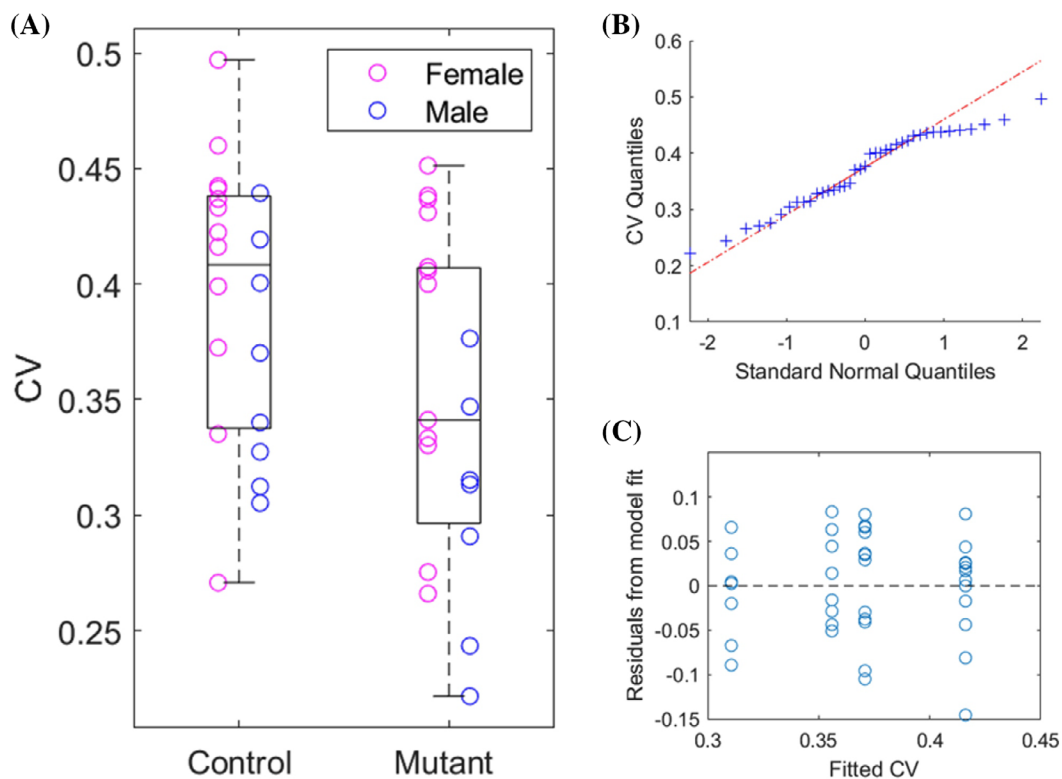


FIGURE 3 CV of IRI distribution is influenced by both sex and genotype. (A) Boxplot showing the CV of the IRI distribution of individual mice (open circles). Linear regression revealed a significant effect of both sex ($p = 0.0036$; $b = 0.060$) and genotype ($p = 0.021$; $b = -0.045$) on CV. The upper, middle, and lower box limits indicate the 75th percentile, median, and 25th percentile, respectively. The whiskers represent $\pm 2.7\sigma$ encompassing 99.3% of the data if the data are normally distributed. (B) Quantile-quantile plot of CV data versus standard normal distribution. Blue “+” signs indicate quantiles, dotted red line represents the plot of the line if data has a perfectly normal distribution. (C) Plot of residuals versus fitted CV. The four groups represented in fitted values are due to the fact that there can only be four possible combinations of the predictor variables sex and genotype. Ideally, residuals are distributed equally amongst groups with no clear trend. Actual data shows no obvious trend, indicating good model fit. Fitted CV values: male mutant, 0.311; male control, 0.356; female mutant, 0.371; female control, 0.416

values were basically normally distributed (Figure 3B) and Breusch-Pagan test confirmed homoscedasticity ($p = 0.65$). ST was originally included as a predictor variable but was not significant ($p = 0.068$) and was removed from the model. After ST was removed, the residual plot in Figure 3C further confirmed appropriate model fit as there was no apparent trend to the residuals. The model was statistically significant ($R^2 = 0.294$; $F_{2,36} = 7.5$; $p = 0.0019$) and there was an effect of both sex ($t_{36} = 3.1$; $p = 0.0036$; $b = 0.060 \pm 0.019$) and genotype on CV ($t_{36} = -2.4$; $p = 0.021$; $b = -0.045 \pm 0.018$). This showed that *Atoh1-En1/2* CKOs had decreased CV as compared to their control littermates and male animals had decreased CV compared to females, as can be seen in Figure 3A. In contrast to our expectations, this indicated that conditional loss of *En1/2* in rhombic lip-derived neurons significantly decreases overall respiratory variability during eupnea, and indicated decreased variability in males compared to females.

Finally, we evaluate intrinsic respiratory rhythmicity. As with rate and CV, CV2 data was also confirmed to be normal (QQ plot in Figure 4B) and homoscedastic ($p = 0.47$, Breusch-Pagan test), and there was no pattern to the residual plot (Figure 4C). Unlike with rate and CV, this model ($R^2 = 0.479$; $F_{3,35} = 10.7$; $p = 3.8 \times 10^{-5}$) showed that ST was a significant predictor of CV2 ($t_{35} = 2.1$; $p = 0.046$)

although the effect size was so small as to be negligible ($b = 4.3 \times 10^{-5} \pm 2.1 \times 10^{-5}$). Similar to CV, linear regression of CV2 revealed a significant effect of both sex and genotype (Figure 4A). *Atoh1-En1/2* CKOs had significantly decreased CV2 values compared to control littermates ($t_{35} = -3.7$; $p < 0.001$; $b = -0.037 \pm 0.010$) and males had significantly decreased CV2 values compared to females ($t_{35} = 2.3$; $p = 0.024$; $b = 0.026 \pm 0.011$). In other words, conditional loss of *En1/2* in the rhombic lip-derived neurons results in reduced variability of intrinsic respiratory rhythmicity during eupnea.

Atoh1-derived neurons are also found in extracerebellar structures, including nuclei implicated in respiratory control, such as the parabrachial nucleus or the lateral reticular nucleus.^{44–46} We evaluated whether loss of *En1/2* in *Atoh1*-derived extracerebellar nuclei showed cell loss similar to the CN in *Atoh1-En1/2* CKO mice compared to controls. Cell counts were performed in the parabrachial nucleus (Figure 5B, i and ii), lateral reticular nucleus (Figure 5B, iii and iv) and the pons (Figure 5B, v and vi) of control and mutant mice expressing nuclear tdTomato in *Atoh1*-derived cells (see methods). Mutant mice suffered from no cell loss in any of the three nuclei (parabrachial nucleus, $U = 6$, $p = 0.6857$; lateral reticular nucleus, $U = 5$, $p = 0.0800$; pons, $U = 4$, $p = 0.3429$) compared to control mice (Figure 5C–E).

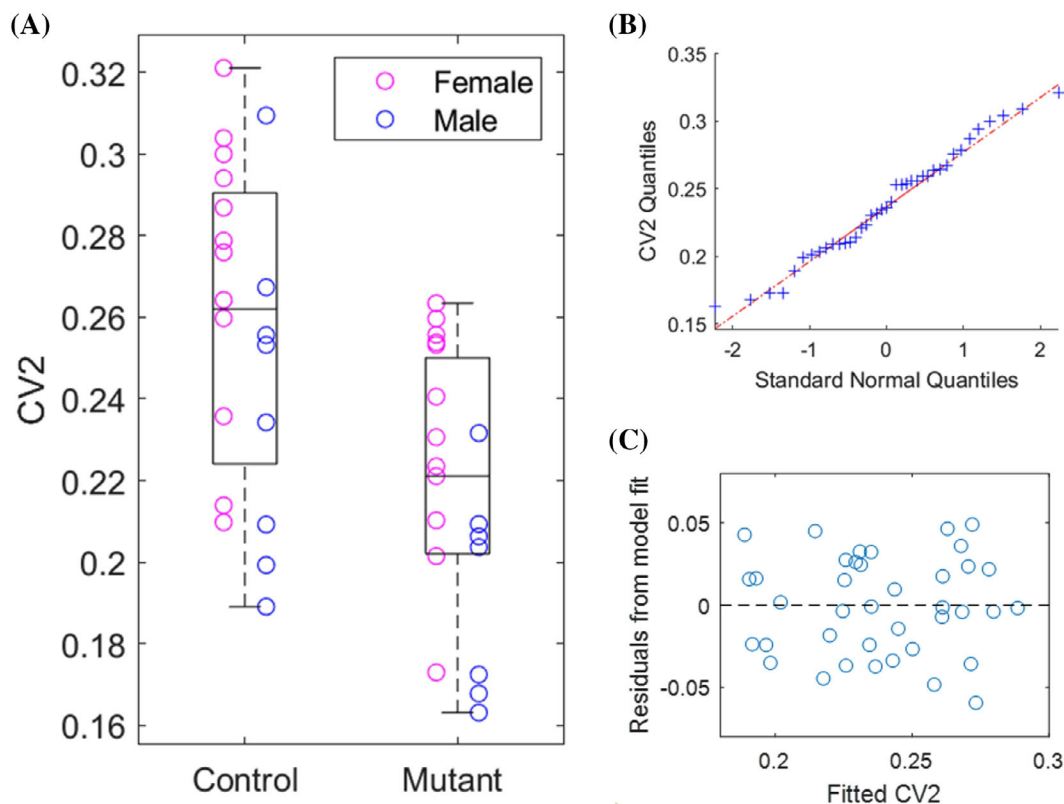


FIGURE 4 Mean CV2 is influenced by both sex and genotype. (A) Boxplot showing the mean CV2 of individual mice (open circles). Linear regression revealed a significant effect of both sex ($p = 0.024$; $b = 0.026$) and genotype ($p < 0.001$; $b = -0.037$) on CV2. Start time was also a significant predictor of CV2 although the effect size was negligible ($p = 0.046$; $b = 4.3 \times 10^{-5}$). The upper, middle, and lower box limits indicate the 75th percentile, median, and 25th percentile, respectively. The whiskers represent $\pm 2.7\sigma$ encompassing 99.3% of the data if the data are normally distributed. (B) Quantile-quantile plot of CV2 data versus standard normal distribution. Blue “+” signs indicate quantiles, dotted red line represents the plot of the line if data has a perfectly normal distribution. (C) Plot of residuals versus fitted CV2. Ideally, residuals are distributed randomly with no clear trend. Actual data shows no obvious trend, indicating good model fit

4 | DISCUSSION

Here we report that *Atoh1-En1/2* CKO mice, compared to control littermates, show altered variability (CV) and intrinsic rhythmicity (CV2) in eupneic breathing, while the average respiratory rate was similar in controls and mutants. Our findings are consistent with previous results from a different mouse model of cerebellar neuropathology, which showed that genetic silencing of PC synaptic transmission in mice caused a decrease in the CV2 of the respiratory rhythm but did not change the average respiratory rate.¹⁵ However, this present

study differed from previous findings in that mutant *Atoh1-En1/2* CKOs also exhibited a decrease in the variability (CV) of eupneic respiratory rhythm.

Our findings are consistent with previous results showing that cerebellar dysfunction caused by loss of Purkinje cell synaptic transmission reduced the CV2 of eupneic respiration.¹⁵ The reduced variability of intrinsic rhythmicity suggests that the healthy cerebellum introduces variability to the respiratory rhythm, and specifically to the intrinsic rhythm, that is, selectively modulating individual IRLs. Specifically, we suggest that modulation of intrinsic rhythmicity serves to adjust select

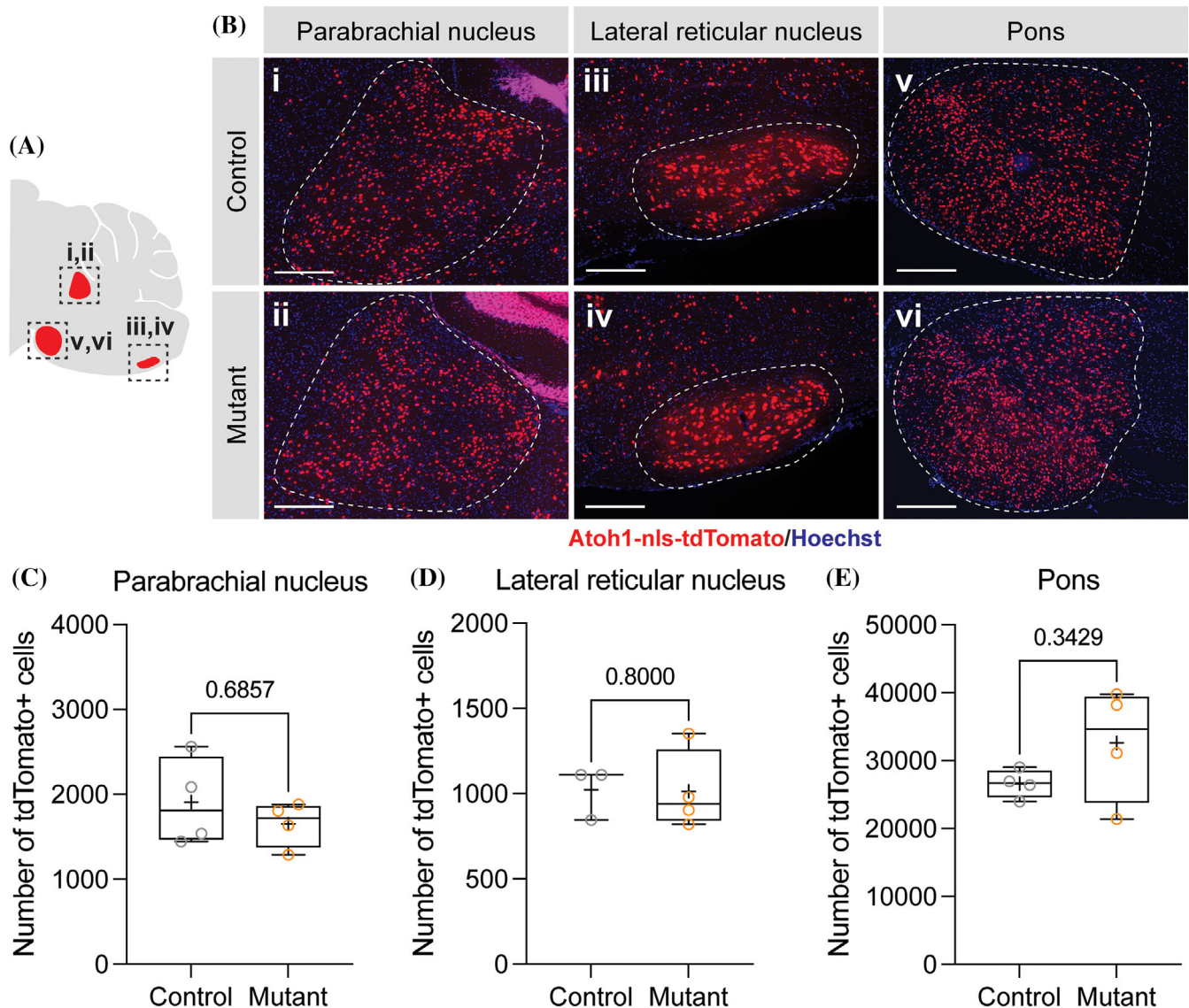


FIGURE 5 *Atoh1*-derived extracerebellar nuclei neurons show no cell loss. (A) Sagittal schematic of *Atoh1*-derived extracerebellar nuclei quantified. i, ii = parabrachial nucleus; iii, iv = lateral reticular nucleus; v, vi = pons. (B) Representative immunofluorescence for *Atoh1*-derived nuclear *tdTomato* (*Atoh1-nls-tdTomato*) and Hoechst for each brain region in control and mutant mice. Dotted white line indicates the corresponding brain region. Scale bar = 250 μ m. (C) Boxplot showing the median and the 1st and 3rd quartile for the cell counts of *Atoh1*-derived *En1/2* neurons expressing *tdTomato* in the parabrachial nucleus of control ($n = 4$) and mutant mice ($n = 4$). The “+” sign indicate the mean and horizontal lines the maximum and minimum values of counts. The number above the bracket represents the p -value (Mann–Whitney U test). (D) As in (C) but for cell counts in the lateral reticular nucleus of control ($n = 3$) and mutant ($n = 4$) mice. (E) As in (C) but for cell counts in the pons of control ($n = 4$) and mutant ($n = 4$) mice

respiratory intervals to coordinate respiration with other orofacial movements such as swallowing, which requires respiration to pause (i.e., the current IRI to be prolonged) while swallowing is completed.⁴⁷

The *Atoh1-En1/2* CKO mutant is known to affect cerebellar granule cells and the eCN in the cerebellum,²⁹ but potentially also affects other *Atoh1*-derived rhombic lip neurons. To address this question, we compared cell counts in three *Atoh1*-derived extracerebellar nuclei and found no cell loss in mutant compared to control mice, suggesting that cell loss in the mutants might thus be limited to or predominantly occur in the CN.

We found sex differences in all three response variables, with females having increased CV and CV2 values and decreased average respiratory rates as compared to males, irrespective of genotype. A modest effect of sex was also found in Liu et al. for both respiratory rate and CV2, although no effect of sex was found for CV in that study.¹⁵ Sex differences in the average respiratory rate are also observed in humans, with males having a slower respiratory rate than females.⁴⁸ A study in rats by Holley et al. suggests that sex-differences in the average respiratory rate change throughout development.⁴⁹ Whether this applies to mice as well and whether or how the CV and CV2 of respiration are altered in sex-specific ways during development remains to be shown.

The vast reciprocal connections between the cerebellum and brainstem provide a putative anatomical substrate for a cerebellar coordination of orofacial and respiratory rhythms.^{16,50–54} Inappropriate coordination of swallowing and respiration can have detrimental effects, as in aspiration pneumonia due to dysphagia in patients with cerebellar ataxia.⁵⁰ Additional studies are needed to test this hypothesis by simultaneously tracking respiration and other rhythmic orofacial behaviors such as licking, swallowing, and whisking.

The recent consensus paper by Bareš et al. emphasized three important aspects of the cerebellum which make it suited for its time-keeping role: microcircuitry, neuronal density, and vast extracerebellar interconnectivity.⁵⁵ The *Atoh1-En1/2* CKO mutants specifically affect cerebellar output neurons and thus connectivity of the cerebellum with downstream structures, rather than an intrinsic cerebellar network deficit. These mutant mice have largely normal neuronal density in the cerebellar cortex, despite its proportionally decreased neuronal number in certain hypoplastic lobules.³² Additionally, the regions of the mCN identified in Lu et al. as projecting to areas containing respiratory generating circuits largely overlap with CN regions which exhibit reduced eCN number in the *Atoh1-En1/2* CKOs.^{16,32} Therefore, we propose that the altered respiratory rhythmicity may be due to a deficit in the highly organized and extensive extracerebellar interconnectivity, in this case between the cerebellum and brain stem circuits involved in respiratory pattern generation. In summary, these results support a role of the cerebellum in eupneic respiration and a possible involvement of the cerebellum in coordinating the respiratory rhythm with other orofacial movements.

ACKNOWLEDGMENTS

We would like to thank the Neuroscience Institute of the University of Tennessee Health Science Center (UTHSC) and the National

Institute of Mental Health for financial support. We also thank Dr. Yu Liu (UTHSC) for supporting the analysis of plethysmograph data, Britany Correia (UTHSC) for assistance with MATLAB and data acquisition, and Shuhua Qi (UTHSC) for maintaining the mouse colony. This work was supported by grants from the NIH to Detlef H. Heck (NIMH R01MH112143), to Angela P. Taylor (NIMH F31MH122068), and to Andrew S. Lee (NICHD T32HD060600). This work was also supported by a grant from the NIH to Alexandra L. Joyner (NIMH R37MH085726) and a National Cancer Institute Cancer Center Support Grant (P30 CA008748-48).

CONFLICT OF INTEREST

The authors declare no conflicts of interest.

AUTHOR CONTRIBUTIONS

Detlef H. Heck and Angela P. Taylor conceived and designed the experiments, wrote and edited the manuscript. Angela P. Taylor performed plethysmograph experiments and performed data and statistical analysis. Alexandra L. Joyner created and provided the mutant mouse, wrote and edited the manuscript. Andrew S. Lee performed tissue imaging experiments and analysis, wrote and edited the manuscript. Patricia J. Goedecke and Elizabeth A. Tolley performed additional statistical analysis, wrote and edited the manuscript.

DATA AVAILABILITY STATEMENT

Data will be available upon request from the corresponding authors.⁵¹

ORCID

Detlef H. Heck  <https://orcid.org/0000-0003-2438-4064>

REFERENCES

1. Bassal M, Bianchi AL. Inspiratory onset or termination induced by electrical stimulation of the brain. *Respir Physiol.* 1982;50(1):23-40.
2. Paton JFR, La Noce A, Sykes RM, et al. Efferent connections of lobule IX of the posterior cerebellar cortex in the rabbit—some functional considerations. *J Auton Nerv Syst.* 1991;36:209-224.
3. Huang Q, Zhou D, St John WM. Cerebellar control of expiratory activities of medullary neurons and spinal nerves. *J Appl Physiol.* 1993;74(4):1934-1940.
4. Gozal D, Hathout GM, Kirlew KA, et al. Localization of putative neural respiratory regions in the human by functional magnetic resonance imaging. *J Appl Physiol.* 1994;76(5):2076-2083.
5. Xu F, Frazier DT. Involvement of the fastigial nuclei in vagally mediated respiratory responses. *J Appl Physiol.* 1997;82(6):1853-1861.
6. Harper RM, Gozal D, Bandler R, Spriggs D, Lee J, Alger J. Regional brain activation in humans during respiratory and blood pressure challenges. *Clin Exp Pharmacol Physiol.* 1998;25(6):483-486.
7. Chen ML, Witmans MB, Tablizo MA, et al. Disordered respiratory control in children with partial cerebellar resections. *Pediatr Pulmonol.* 2005;40(1):88-91.
8. Macey PM, Woo MA, Macey KE, et al. Hypoxia reveals posterior thalamic, cerebellar, midbrain, and limbic deficits in congenital central hypoventilation syndrome. *J Appl Physiol.* 2005;98(3):958-969.
9. Feldman JL, Del Negro CA. Looking for inspiration: new perspectives on respiratory rhythm. *Nat Rev Neurosci.* 2006;7(3):232-242.
10. Rector DM, Richard CA, Harper RM. Cerebellar fastigial nuclei activity during blood pressure challenges. *J Appl Physiol.* 2006;101(2):549-555.

11. Moruzzi G. Paleocerebellar inhibition of vasomotor and respiratory carotid sinus reflexes. *J Neurophysiol.* 1940;3(1):20-32.
12. Xu F, Owen J, Frazier DT. Hypoxic respiratory responses attenuated by ablation of the cerebellum or fastigial nuclei. *J Appl Physiol.* 1995; 79(4):1181-1189.
13. Parsons LM, Egan G, Liotti M, et al. Neuroimaging evidence implicating cerebellum in the experience of hypercapnia and hunger for air. *Proc Natl Acad Sci.* 2001;98(4):2041-2046.
14. Calton MA, Howard JR, Harper RM, Goldowitz D, Mittleman G. The cerebellum and SIDS: disordered breathing in a mouse model of developmental cerebellar Purkinje cell loss during recovery from hypercarbia. *Front Neurol.* 2016;7:78.
15. Liu Y, Qi S, Thomas F, et al. Loss of cerebellar function selectively affects intrinsic rhythmicity of eupneic breathing. *Biol Open.* 2020; 9(4):bio048785.
16. Lu L, Cao Y, Tokita K, Heck DH, Boughter JD. Medial cerebellar nuclear projections and activity patterns link cerebellar output to orofacial and respiratory behavior. *Front Neural Circuits.* 2013;7:56.
17. Romano V, Reddington AL, Cazzanelli S, et al. Functional convergence of autonomic and sensorimotor processing in the lateral cerebellum. *Cell Rep.* 2020;32(1):7867.
18. Leto K, Arancillo M, Becker EB, et al. Consensus paper: cerebellar development. *Cerebellum.* 2016;15(6):789-828.
19. White JJ, Arancillo M, Stay TL, et al. Cerebellar zonal patterning relies on purkinje cell neurotransmission. *J Neurosci.* 2014;34(24):8231-8245.
20. Holt GR, Softky WR, Koch C, Douglas RJ. Comparison of discharge variability in vitro and in vivo in cat visual cortex neurons. *J Neurophysiol.* 1996;75(5):1806-1814.
21. *Neuroscience.* 2nd ed. Sinauer Associates; 2001.
22. Sillitoe RV, Joyner AL. Morphology, molecular codes, and circuitry produce the three-dimensional complexity of the cerebellum. *Ann Rev Cell Dev Biol.* 2007;23:549-577.
23. Fujita H, Kodama T, du Lac S. Modular output circuits of the fastigial nucleus for diverse motor and nonmotor functions of the cerebellar vermis. *Elife.* 2020;9:e58613.
24. Kobschull JM, Richman EB, Ringach N, et al. Cerebellar nuclei evolved by repeatedly duplicating a conserved cell-type set. *Science.* 2020; 370:6523.
25. Sergievskii MV, Kireeva N. Reciprocal connections of respiratory center nuclei. *O Vzaïmnykh Svïaziakh lader dykhatel'nogo Tsentra.* 1980; 90:1639-1642.
26. Bystrzycka EK, Nail BS. The source of the respiratory drive to nasolabial motoneurons in the rabbit; a HRP study. *Brain Res.* 1983; 266(2):183-191.
27. Dobbins EG, Feldman JL. Brainstem network controlling descending drive to phrenic motoneurons in rat. *J Comp Neurol.* 1994;347(1):64-86.
28. Zhang Z, Xu F, Frazier DT. Role of the Botzinger complex in fastigial nucleus-mediated respiratory responses. *Anat Rec.* 1999;254(4):542-548.
29. Orvis GD, Hartzell AL, Smith JB, et al. The engrailed homeobox genes are required in multiple cell lineages to coordinate sequential formation of fissures and growth of the cerebellum. *Dev Biol.* 2012;367(1): 25-39.
30. Wilson SL, Kalinovsky A, Orvis GD, Joyner AL. Spatially restricted and developmentally dynamic expression of engrailed genes in multiple cerebellar cell types. *Cerebellum.* 2011;10(3):356-372.
31. Legue E, Gottshall JL, Jaumouille E, et al. Differential timing of granule cell production during cerebellum development underlies generation of the foliation pattern. *Neural Dev.* 2016;11(1):17.
32. Willett RT, Bayin NS, Lee AS, et al. Cerebellar nuclei excitatory neurons regulate developmental scaling of presynaptic Purkinje cell number and organ growth. *Elife.* 2019;8:e50617.
33. Sillitoe RV, Stephen D, Lao Z, Joyner AL. Engrailed homeobox genes determine the organization of Purkinje cell sagittal stripe gene expression in the adult cerebellum. *J Neurosci.* 2008;28(47):12150-12162.
34. Sillitoe RV, Vogel MW, Joyner AL. Engrailed homeobox genes regulate establishment of the cerebellar afferent circuit map. *J Neurosci.* 2010;30(30):15-24.
35. Cheng Y, Sudarov A, Szulc KU, et al. The engrailed homeobox genes determine the different foliation patterns in the vermis and hemispheres of the mammalian cerebellum. *Development.* 2010;137(3):519-529.
36. Van der Heijden ME, Zoghbi HY. Loss of Atoh1 from neurons regulating hypoxic and hypercapnic chemoresponses causes neonatal respiratory failure in mice. *Elife.* 2018;7:8455.
37. Flurkey K, Curren J, Harrison DE. Chapter 20 - Mouse models in aging research. In: Fox JG, Davisson MT, Quimby FW, Barthold SW, Newcomer CE, Smith AL, eds. *The Mouse in Biomedical Research.* 2nd ed. Academic Press; 2007:637-672.
38. Madisen L, Zwingman TA, Sunkin SM, et al. A robust and high-throughput Cre reporting and characterization system for the whole mouse brain. *Nat Neurosci.* 2010;13(1):133-140.
39. Lim R, Zavou MJ, Milton PL, et al. Measuring respiratory function in mice using unrestrained whole-body plethysmography. *J Vis Exp.* 2014;90:e51755.
40. Wesson DW, Donahou TN, Johnson MO, Wachowiak M. Sniffing behavior of mice during performance in odor-guided tasks. *Chem Senses.* 2008;33(7):581-596.
41. Wesson DW, Varga-Wesson AG, Borkowski AH, Wilson DA. Respiratory and sniffing behaviors throughout adulthood and aging in mice. *Behav Brain Res.* 2011;223(1):99-106.
42. Breusch TS, Pagan AR. A simple test for heteroscedasticity and random coefficient variation. *Econometrica.* 1979;47(5):1287-1294.
43. Magris MBreusch-Pagan Test. MATLAB central file exchange. Accessed 22 July 2020, 2020. <https://www.mathworks.com/matlabcentral/fileexchange/75340-breusch-pagan-test>
44. Chamberlin NL, Saper CB. Topographic organization of respiratory responses to glutamate microstimulation of the parabrachial nucleus in the rat. *J Neurosci.* 1994;14(11):6500-6510.
45. Smotherman M, Schwartz C, Metzner W. Chapter 9.2 - Vocal-respiratory interactions in the parabrachial nucleus. In: Brudzynski SM, ed. *Handbook of Behavioral Neuroscience.* Elsevier; 2010:383-392.
46. Alstermark B, Ekerot CF. The lateral reticular nucleus: a precerebellar centre providing the cerebellum with overview and integration of motor functions at systems level. A new hypothesis. *J Physiol.* 2013; 591(22):5453-5458.
47. Liu Y, Qi S, Thomas F, et al. Loss of cerebellar function selectively affects intrinsic rhythmicity of eupneic breathing. *Biol Open.* 2020.9(4).
48. LoMauro A, Aliverti A. Sex differences in respiratory function. *Breathe.* 2018;14(2):131-140.
49. Holley HS, Behan M, Wenninger JM. Age and sex differences in the ventilatory response to hypoxia and hypercapnia in awake neonatal, prepubertal and young adult rats. *Respir Physiol Neurobiol.* 2012;180(1):79-87.
50. Ramio-Torrentia L, Gomez E, Genis D. Swallowing in degenerative ataxias. *J Neurol.* 2006;253(7):875-881.
51. Bryant JL, Roy S, Boughter JD, et al. A proposed new function of the mouse cerebellum: temporal modulation of brain stem pattern generator activity. *Soc Neurosci Abstr.* 2007;78:17.
52. Hardemark Cedborg AI, Sundman E, Bodén K, et al. Co-ordination of spontaneous swallowing with respiratory airflow and diaphragmatic and abdominal muscle activity in healthy adult humans. *Exp Physiol.* 2009;94(4):459-468.
53. Bryant JL, Boughter JD, Gong S, LeDoux MS, Heck DH. Cerebellar cortical output encodes temporal aspects of rhythmic licking movements and is necessary for normal licking frequency. *Eur J Neurosci.* 2010;32(1):41-52.
54. Yagi N, Oku Y, Nagami S, et al. Inappropriate timing of swallow in the respiratory cycle causes breathing-swallowing discoordination. *Front Physiol.* 2017;8:676.

55. Bareš M, Apps R, Avanzino L, et al. Consensus paper: decoding the contributions of the cerebellum as a time machine. From neurons to clinical applications. *Cerebellum*. 2019;18(2):266-286.

SUPPORTING INFORMATION

Additional supporting information may be found in the online version of the article at the publisher's website.

How to cite this article: Taylor AP, Lee AS, Goedecke PJ, Tolley EA, Joyner AL, Heck DH. Conditional loss of *Engrailed1/2* in *Atoh1*-derived excitatory cerebellar nuclear neurons impairs eupneic respiration in mice. *Genes, Brain and Behavior*. 2022;21(2):e12788. doi:10.1111/gbb.12788